Stability and Hopf bifurcations in an inverted pendulum

James A. Blackburn, H. J. T. Smith and N. Gro/nbech-Jensen

Citation: American Journal of Physics **60**, 903 (1992); doi: 10.1119/1.17011
View online: https://doi.org/10.1119/1.17011
View Table of Contents: https://aapt.scitation.org/toc/ajp/60/10
Published by the American Association of Physics Teachers

Stability and Hopf bifurcations in an inverted pendulum

James A. Blackburn
Department of Physics and Computing, Wilfrid Laurier University, Waterloo, Ontario, Canada

H. J. T. Smith
Physics Department, University of Waterloo, Waterloo, Ontario, Canada

N. Grønbech-Jensen[a)]
Physics Laboratory I, Technical University of Denmark, Lyngby, Denmark

(Received 15 July 1991; accepted 6 April 1992)

The inverted state of a simple pendulum is a configuration of unstable equilibrium. This instability may be removed if the pivot is harmonically displaced up and down with appropriate frequency and amplitude. Numerical simulations are employed to investigate the stable domains of the system. The associated basins of attraction, extracted by interpolated cell mapping, are seen to be fractal. Loss of stability at high excitation amplitudes is observed to follow a Hopf bifurcation.

I. INTRODUCTION

A simple pendulum, consisting of a mass m at a distance r from a pivot, has two equilibrium configurations: m located in the *down* or the *up* position. The down position is obviously stable, while the vertical orientation is clearly unstable. It is known that this second equilibrium state can be made stable by subjecting the pivot itself to a harmonic vertical oscillation of appropriate frequency and amplitude. This rather remarkable result, which seems somewhat counterintuitive, is not commonly discussed in texts on classical mechanics,[1] although it has appeared from time to time in the scientific literature.[2–7] In a variant of this problem, Miles[8] recently showed that suitably chosen *direct excitation* (that is, a harmonic applied *torque* rather than a periodic displacement of the pivot) could produce motion with symmetry about the up, rather than down, orientation of the pendulum. An examination of the phase plane plot in Ref. 8 reveals that these "inverted oscillations" have large amplitudes (greater than π), meaning that a quasistationary inverted state is not achieved under this particular form of direct excitation.

In this work, we endeavor to provide a coherent picture of the properties of the inverted state of a pendulum whose pivot is subjected to harmonic vertical displacement. We begin by summarizing the two principal theoretical approaches to the problem: an approximation of the equation of motion by the Mathieu equation, and a phenomenological model based on an effective potential. Numerical simulations are then employed to investigate the manner in which the inverted position destabilizes as the amplitude of the pivot oscillation is increased beyond a critical value. We find that the stationary vertical state undergoes a Hopf bifurcation leading to a flutter mode. Finally, using interpolated cell mapping, basins of attraction are computed for operating points both inside the domain of stability, and in the flutter zone.

II. THEORY

The pendulum consists of a mass m fixed at a distance r from a pivot which is subjected to a vertical oscillation $y=A\cos(\omega t)$. As indicated in Fig. 1, let θ be the angular coordinate of m measured counterclockwise from the down position, and ϕ be the complementary displacement measured clockwise from the up orientation ($\theta+\phi=\pi$). In experimental apparatus,[9] additional components may be attached to the pivot axis and co-rotate with the mass m; hence let the moment of inertia of these components be denoted I^*. The general equation of motion, including velocity dependent damping, is

$$I\frac{d^2\theta}{dt^2}+b\frac{d\theta}{dt}+mr[g-A\omega^2\cos(\omega t)]\sin\theta=0, \tag{1}$$

where b is a damping coefficient and $I=I^*+mr^2$ is the total moment of inertia of the system. The undamped natural frequency ω_0 is given by $\omega_0^2=mgr/I$. If time is normalized according to the transformation $\omega t\rightarrow t$, then we obtain

$$\frac{d^2\theta}{dt^2}+\left(\frac{1}{\Omega Q}\right)\frac{d\theta}{dt}+\left[\left(\frac{1}{\Omega^2}\right)-\left(\frac{A}{r}\frac{mr^2}{I}\right)\cos(t)\right]\sin(\theta)=0, \tag{2}$$

where $Q=\omega_0 I/b$ and $\Omega=\omega/\omega_0$. For the alternate coordinate ϕ, the equation of motion is

$$\frac{d^2\phi}{dt^2}+\left(\frac{1}{\Omega Q}\right)\frac{d\phi}{dt}+\left[\left(\frac{-1}{\Omega^2}\right)+\left(\frac{A}{r}\frac{mr^2}{I}\right)\cos(t)\right]\sin(\phi)=0. \tag{3}$$

A. Mathieu equation

Equilibrium about the down position can be evaluated by determining the stability of solutions of Eq. (2) with $\sin(\theta)\approx\theta$. In a similar fashion, the inverted position may be treated by assuming $\sin(\phi)\approx\phi$ in Eq. (3). In either case, the equations take the canonical form,

$$\frac{d^2\psi}{dt^2}+\beta\frac{d\psi}{dt}+[\delta+\epsilon\cos(t)]\psi=0, \tag{4}$$

with $\psi=\theta$ or ϕ, $\beta=(\Omega Q)^{-1}$, $\delta=+/-\Omega^{-2}$, and $\epsilon=-/+(A/r)(mr^2/I)$. We shall be interested in parameter domains $Q>5$ and $\Omega>5$; the β term may then be neglected and Eq. (4) will take the form of the Mathieu equation. The sign of δ is important, as will be seen, but the sign of ϵ has no effect on the stability of the system. Henceforth, ϵ will be treated as a positive quantity.

The issue of the stability of either orientation of the pendulum (inverted with $\phi\approx 0$ and $\delta<0$, or noninverted with $\theta\approx 0$ and $\delta>0$) can now be addressed with reference to the general literature available on the Mathieu equation;

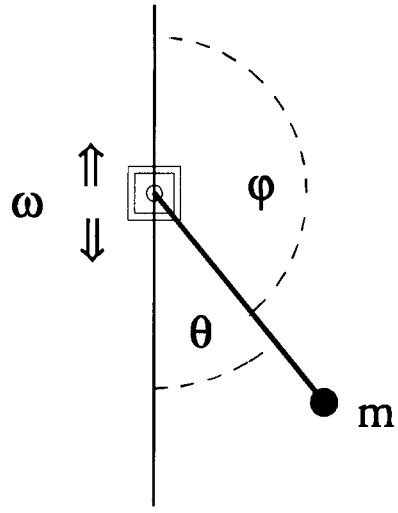

Fig. 1. Schematic of a simple pendulum whose point of suspension undergoes vertical oscillations.

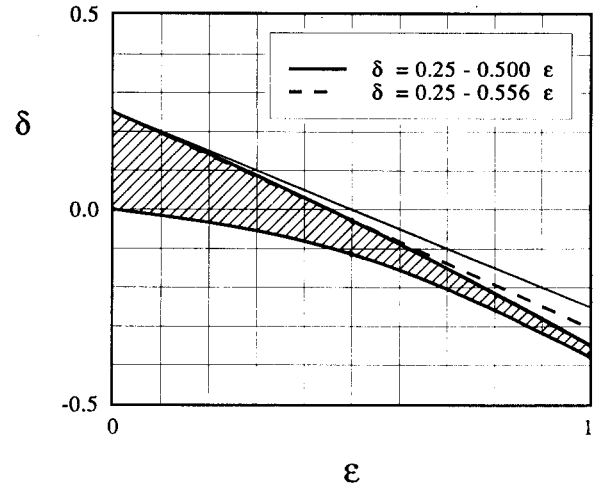

Fig. 3. Expanded view of the first stability zone and the two linear approximations to the upper boundary.

the properties of the (ϵ,δ) plane shown in Fig. 2 are a standard result.[3,6,10–12]

Useful approximations for the stability boundaries at small ϵ are given in Refs. (10) and (11). For the first stable region in Fig. 2, they are $\delta\approx-(1/2)\epsilon^2$ and $\delta\approx 1/4-(1/2)\epsilon$. At $\epsilon=0.5$, this latter expression yields $\delta=0$. The exact value[10] is -0.02756. An improved approximation which is valid over a larger range of ϵ is that of a straight line passing through $\delta=0.25$ at $\epsilon=0$, and $\delta=-0.028$ at $\epsilon=0.5$; hence, $\delta=1/4-0.556\epsilon$. These two linear functions are plotted in an expanded view of the first stability zone, shown in Fig. 3.

In terms of the more physical parameters (ϵ,Ω), the first stable region in the *inverted case* $(\delta=-\Omega^{-2})$ thus lies between the two curves:

$$\epsilon=\sqrt{2}/\Omega, \tag{5}$$

$$\epsilon=0.450+1.799/\Omega^2. \tag{6}$$

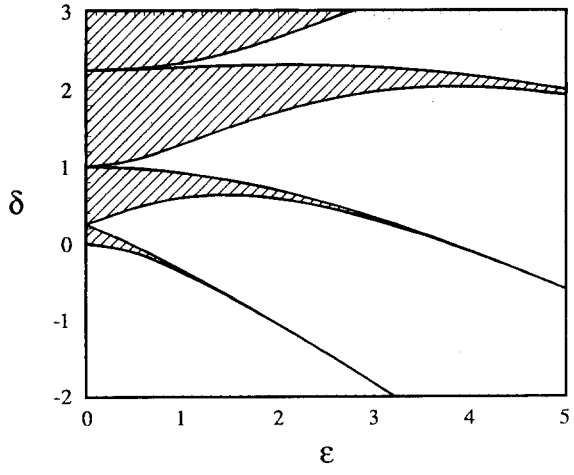

Fig. 2. Stability diagram for the Mathieu equation. The vertical coordinate is the reciprocal normalized drive frequency: $\delta=(\omega_0/\omega)^2$; the horizontal coordinate is the normalized drive amplitude: $\epsilon=(A/r)(mr^2/I)$. The regions of stability are shaded.

These equations[13] are plotted in Fig. 4 as solid lines. As an example, suppose the pivot is oscillating at a frequency which is 11 times the natural frequency ω_0. The two squares in the figure indicate that the inverted position will be stable provided the amplitude of these oscillations lies between $\epsilon=0.129$ and 0.465. For the *noninverted case* $(\delta=+\Omega^{-2})$, the stable region lies between $\epsilon=0$ and

$$\epsilon=0.450-1.799/\Omega^2,$$

in other words, between the vertical axis and the dotted curve in Fig. 4. The shaded region in the figure thus represents that portion of (ϵ,Ω) space for which *both* up and down states should be stable.

B. Effective potential

In their classic text on mechanics,[14] Landau and Lifshitz briefly indicate an approach to the problem of the inverted

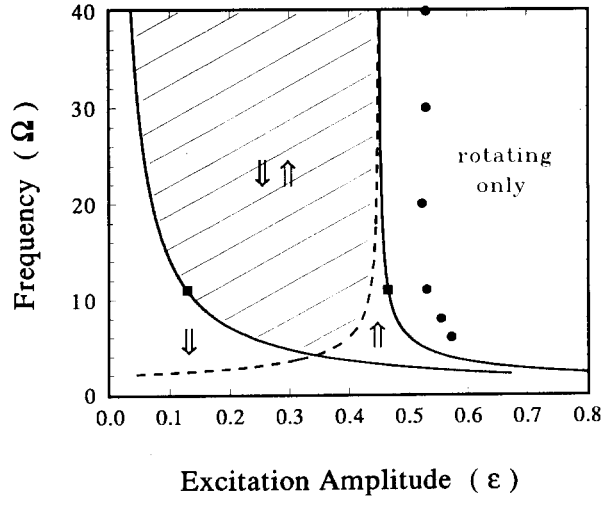

Fig. 4. Stability diagram for the pendulum. Up and down arrows signify regions of stability for the inverted and normal configurations, respectively. Dots denote points that lie along the upper boundary of the flutter zone and were determined from numerical simulations.

pendulum. Following their method, and assuming that $\Omega \gg 1$ in Eq. (2), the phase is separated into "slow" (Θ) and "fast" (ξ) components: $\theta = \Theta + \xi$. From Eq. (2), we obtain

$$\ddot{\xi} + \frac{1}{\Omega Q}\dot{\xi} + \frac{1}{\Omega^2}\xi \cos\Theta - \epsilon \cos t \sin\Theta = 0, \tag{7}$$

$$\ddot{\Theta} + \frac{1}{\Omega Q}\dot{\Theta} + \frac{1}{\Omega^2}\sin\Theta - \epsilon\langle \xi \cos t\rangle \cos\Theta = 0, \tag{8}$$

where ξ is assumed small, overdots indicate time derivatives, and the brackets $\langle\ \rangle$ denote the dc part of the argument. The solution $\xi(t)$ to the linear Eq. (7) is found immediately to be

$$\xi(t) = \frac{\epsilon \sin\Theta}{(\delta^* \cos\Theta - 1)^2 + \beta^2}\left[(\delta^* \cos\Theta - 1)\cos t + \beta \sin t\right], \tag{9}$$

with $\delta^* = |\delta|$. Inserting this into Eq. (8), we obtain for the slowly varying component of θ:

$$\ddot{\Theta} + \beta\dot{\Theta} + \delta^* \sin\Theta - \frac{\epsilon^2}{4}\left(\frac{\delta^* \cos\Theta - 1}{(\delta^* \cos\Theta - 1)^2 + \beta^2}\right)\sin(2\Theta) = 0. \tag{10}$$

Clearly there is an effective dc potential for the slow motion, given by

$$E_{\text{eff}}(\Theta) = \delta^*\left[1 - \cos\Theta + \frac{\epsilon^2}{8\delta^*}\left(\frac{1 - \delta^* \cos\Theta}{(1 - \delta^* \cos\Theta)^2 + \beta^2}\right)[1 - \cos(2\Theta)]\right], \tag{11}$$

which is for large driving frequencies and relatively low losses very well approximated by,

$$E_{\text{eff}}(\Theta) \approx \frac{1}{\Omega^2}\left[1 - \cos\Theta + \frac{1}{2}\left(\frac{\epsilon\Omega}{2}\right)^2 (1 - \cos 2\Theta)\right]. \tag{12}$$

This effective potential is plotted in Fig. 5 for a number of ϵ values. When ϵ is large enough, a potential well develops at $\Theta = \pi$, resulting in a stable inverted state. From Eq. (12), the condition for this to occur is seen to be

$$\left.\frac{\partial^2 E_{\text{eff}}}{\partial \Theta^2}\right|_{\Theta=\pi} > 0 \Rightarrow \frac{(\Omega\epsilon)^2}{2} > 1. \tag{13}$$

This relationship between ϵ and Ω is identical to the expression given on p. 95 of Landau and Lifshitz,[14] and to the previously quoted result [Eq. (5)] for the lower stability boundary of the Mathieu equation. The effective potential method also concludes, as noted by Landau and Lifshitz, that the noninverted state $\Theta = 0$ is always stable. However, it is important to note that, in contrast to the earlier analysis, the effective potential method does not yield *upper* stability boundaries in the (ϵ, Ω) plane and so leaves unanswered the question of possible destabilization at larger excitation amplitudes. In the earlier treatment of the Mathieu equation, it was seen that the noninverted state ($\delta > 0$) will indeed become unstable if, for any chosen frequency Ω, ϵ is increased sufficiently.

While the effective potential method clearly provides only a partial picture of the stability properties of this pendulum, it does in fact yield some results not available from the Mathieu equation (which contains no dissipation term). For example, from Eq. (11) it is apparent that finite damping enhances the stability of the inverted state, but that this influence is small since the correction is of second order in $(\Omega Q)^{-1}$. The width of the potential well at $\Theta = \pi$ may be found by setting $\partial E_{\text{eff}}/\partial\Theta = 0$. The rims of the well are located at the two angles which satisfy $\cos\Theta = -2/(\epsilon\Omega)^2$. If the drive frequency is fixed at some value and the excitation amplitude is increased, then the well will become wider. This in turn implies that larger initial displacements from the vertical would still lead to the stationary inverted state. Such an effect is indeed observed in the simulation results which are discussed next. For large ϵ and Ω, the well has a limiting maximum range extending from $\Theta = \pi/2$ to $3\pi/2$ (90 deg on either side of the vertical).

Finally, we note that the equation of motion arising from the effective potential approach is valid for all phase angles of the pendulum, whereas the Mathieu equation treatment is restricted to small amplitude behavior around some chosen angle. Hence, a study of the *rotating* state of the pendulum under the influence of a fast parametric force can only be carried out with the approximations of the effective potential.

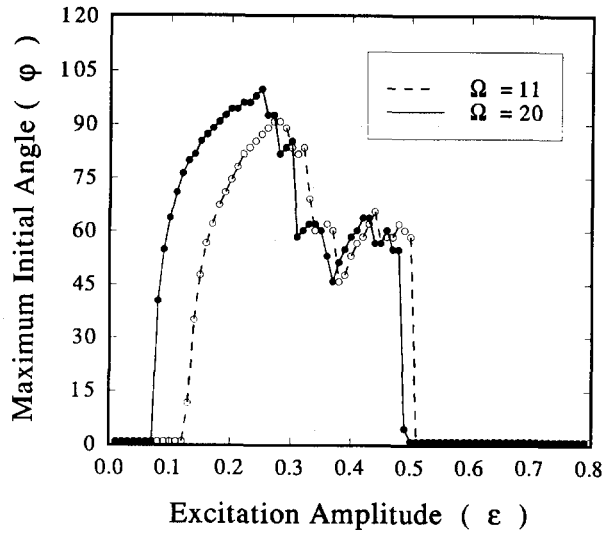

Fig. 5. Effective potential as a function Θ for $\Omega = 11$. The values of ϵ are 0.05, 0.13, 0.20, and 0.30, beginning with the lowest curve.

III. SIMULATION RESULTS

A fourth-order Runge Kutta routine was employed to compute numerical solutions of Eq. (2). All calculations were carried out in double precision arithmetic. The integration time step generally was chosen to be 0.01 of the drive period, although in certain circumstances it was set at 0.001 of a period. Simulations quickly revealed that a stable inverted state could be easily achieved. If the pendulum was released from rest at a small enough initial angle relative to the vertical, the subsequent motion typically damped toward the final state $\theta = \pi$. In fact, for given Q, Ω, and ϵ it was possible to determine a maximum release angle beyond which the stationary inverted state was not achieved. In effect, this procedure probes the width of the potential well, as discussed in the previous section. It

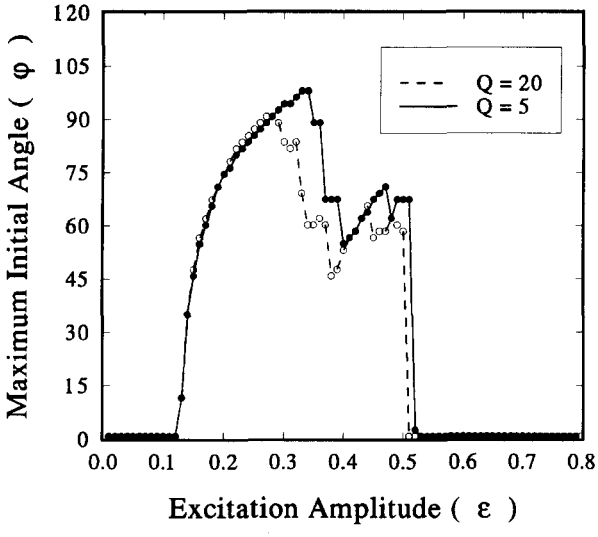

Fig. 6. Plot of maximum release angle (measured from the top) for which a stationary or bounded inverted state results, as a function of the amplitude of the pivot excitation. Data are presented for two drive frequencies, both sets with $Q=20$.

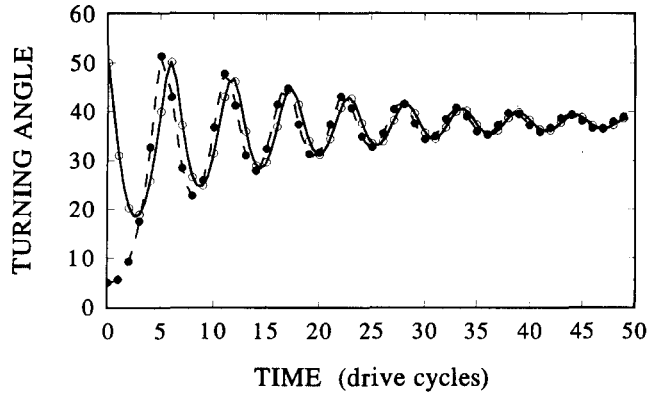

Fig. 8. Damped approach of phase plane orbit toward a state in which the pendulum flutters regularly from side to side with an amplitude of about 40 deg. Note that two very different starting points lead to the same final motion. Parameters were $Q=5$, $\Omega=11$, $\epsilon=0.50$.

was also found that for a given Ω, there was a maximum ϵ above which only rotational motion occurred. For values of ϵ just below this maximum, the pendulum did not come to rest in the up position, no matter how small the release angle, but instead the motion remained bounded in the vicinity of $\theta=\pi$.

Simulation data are presented in Fig. 6 for two different values of excitation frequency. The relatively large allowable initial displacement from the vertical, which was always in excess of 45 deg, indicates the robustness of the inverted state. For $\Omega=11$, stability commences at $\epsilon\approx0.12$, in good agreement with the theoretical prediction from the Mathieu equation of $\epsilon=\sqrt{2}/\Omega$. It is also readily apparent from Fig. 6 that for larger Ω, although the end points of the stability range each shift to smaller values of ϵ, the magnitude of the range increases. This is consistent with the predictions of Fig. 4. Figure 7 illustrates the near independence of the stability zone with respect to the damping parameter Q.

As noted earlier, for values of ϵ slightly below the upper end point of the range for bounded motion, a new type of behavior was observed. After release from rest at some initial angle θ_0, the phase plane (θ, $d\theta/dt$) orbit would take on a double-lobed form that would exhibit damped pulsations leading to a final limit cycle. A typical plot of successive maximum angular displacements (which occur at $d\theta/dt=0$) of such an orbit is shown in Fig. 8, where it can be seen that the pendulum ultimately settled into a limit cycle that extended approximately 40 deg on either side of the inverted position. The figure also demonstrates that this final condition is independent of the release angle, and so is a function only of the parameters Ω and ϵ.

Several limit cycles are shown in Fig. 9. Each orbit was completed in exactly two periods of the vertical excitation (hence, there is phase locking at half the external drive frequency). This type of motion could be described as a *flutter mode* since the pendulum is oscillating about the vertical at half the drive frequency. From the data in this

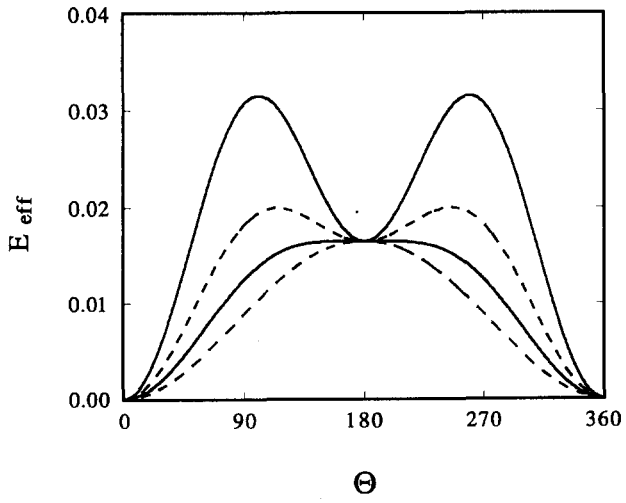

Fig. 7. Effect of damping parameter Q on the maximum release angle at which an inverted state is still reached for $\Omega=11$.

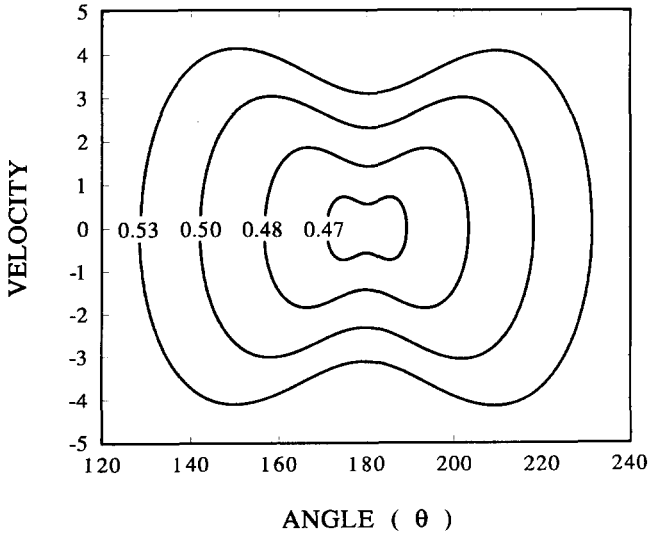

Fig. 9. Limit cycles for $Q=5$, $\Omega=11$ at four different drive amplitudes ϵ.

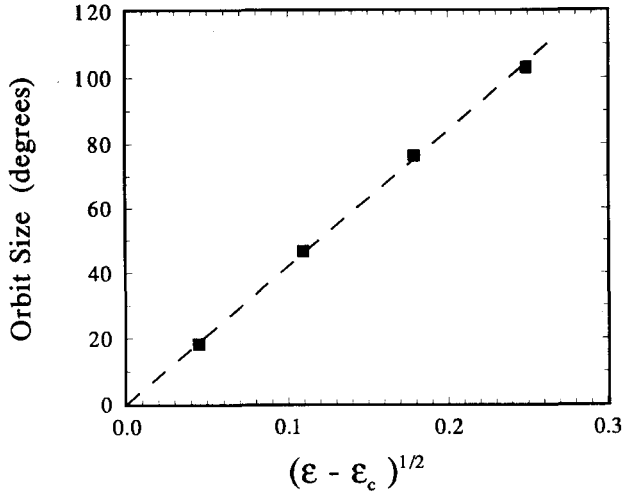

Fig. 10. Limit cycle size as a function of $(\epsilon-\epsilon_c)^{1/2}$.

figure, it can be seen that the flutter amplitude becomes zero at a critical normalized drive ϵ_c of 0.468. Note that this ϵ_c is just the value of ϵ at the upper Mathieu stability boundary as defined by the expression $\epsilon=0.450+1.799/\Omega^2$ $(=0.465)$. Figure 10 displays the dependence of the flutter amplitude on the square root of $(\epsilon-\epsilon_c)$. The linearity of this relationship is a typical of a Hopf bifurcation.[15,16]

The simulation results for $\Omega=11$ may be summarized as follows. For $0.12<\epsilon<\epsilon_c$, a stationary inverted state would be achieved. For $\epsilon_c<\epsilon<0.53$, the pendulum fluttered about the vertical with an amplitude which increased as ϵ approached the maximum value of 0.53, at which point the inverted state became completely unstable and the pendulum rotated (recall from Fig. 4 that the vertically down position had already become unstable at a somewhat smaller value of ϵ and was thus unavailable to the system).

Generally, therefore, the inverted state of the pendulum fully destabilizes by first passing through a Hopf bifurcation which results in increasing flutter amplitudes. The zone in which this transition takes place lies just above the upper stability boundary as determined from the Mathieu equation (see Fig. 4).

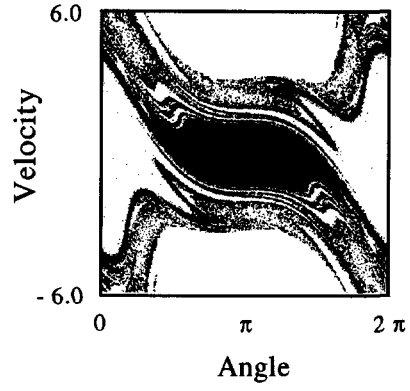

Fig. 12. Basin of attraction well within the stability region of the inverted state: $Q=5$, $\epsilon=0.300$, $\Omega=11$.

IV. BASINS OF ATTRACTION

Depending on the parameters (ϵ,Ω) and initial conditions $(\theta,d\theta/dt)_0$, the pendulum will, after an interval in which transients decay, settle into one out of a number of possible dynamic states. These include the inverted and noninverted configurations, as well as various spinning modes. The set of initial conditions leading to a given equilibrium state (attractor) is its basin of attraction. The most direct way of determining a basin of attraction is to systematically select $(\theta,d\theta/dt)_0$ from a large array of values, and then by integrating the equation of motion discover whether each initial condition leads to the particular attractor. Detailed basin maps can require up to 1000×1000 arrays of starting values, posing severe computational demands. An efficient algorithm known as interpolated cell mapping[17,18] can generate high resolution basins 30 to 50 times faster. ICM was employed to calculate the basins discussed below.

Figure 11 illustrates the basin of attraction for the inverted state of the pendulum operating just above the lower stability boundary. As is typically the case, there is a dense basin core surrounded by fractal layers. The residue in the $(\theta,d\theta/dt)$ plane (white areas) represents a mixture of basins for other states: noninverted and spinning. As ϵ is increased to a value (0.300) well within the stability region shown in Fig. 4, the basin expands (Fig. 12). The basin in Fig. 13 occurs just *below* the upper Mathieu stability

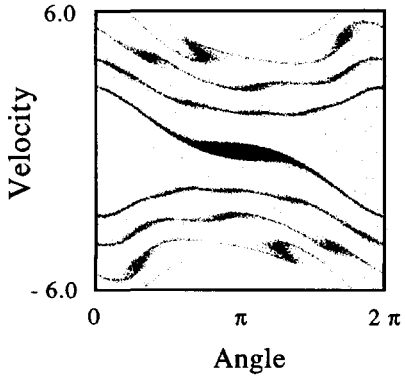

Fig. 11. Basin of attraction for the inverted state determined by interpolated cell mapping for $Q=5$, $\epsilon=0.150$ and $\Omega=11$.

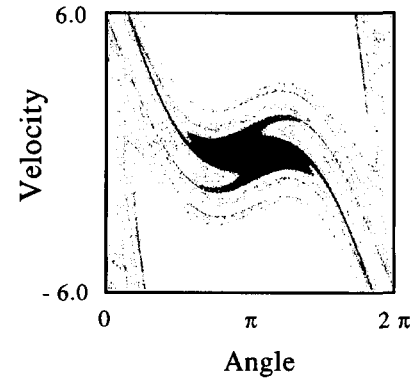

Fig. 13. Basin of attraction of the inverted state just below the upper stability boundary. $Q=5$, $\epsilon=0.460$, $\Omega=11$.

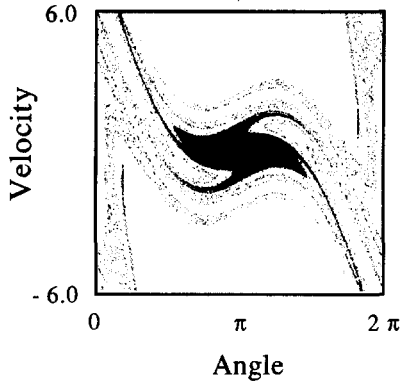

Fig. 14. Basin of attraction of the flutter mode for the inverted state just after the Hopf bifurcation. $Q=5$, $\epsilon=0.470$, $\Omega=11$.

boundary, while that in Fig. 14 is for the flutter mode lying just *above* it (i.e., immediately following the Hopf bifurcation). Figs. 13 and 14 show that, at a Hopf bifurcation, the basin of the stable inverted state is spontaneously converted into an identical basin for the flutter mode. Finally, Fig. 15 illustrates the evolution of the basin for the flutter mode as complete instability is approached. At slightly larger ϵ this basin disappears, since then only spinning states exist.

V. CONCLUSIONS

The simple pendulum is a very old device, yet it is a paradigm of contemporary nonlinear dynamics.[19] When excited by a harmonic torque, it is a mechanical analog of a superconducting Josephson junction.[9] Most significant, perhaps, is the appearance of chaos under a wide range of drive conditions.[20] The particular system considered here—a pendulum with a vertically oscillating point of suspension—also exhibits a number of interesting properties, especially the stability of the inverted state. This process of "dynamic stabilization," as noted by Michaelis[7] and Friedman *et al.*,[6] plays an important role in other, quite different physical phenomena such as quadrupole mass filters and various types of plasma confinement. An analysis of the dynamics brings into play numerical simulations, stability theory of the Mathieu equation, approximation methods, the interpolated cell mapping algorithm for determining basins of attraction, and Hopf bifurcations. Although not the subject of this paper, chaotic motion can occur at lower excitation frequencies.[21]

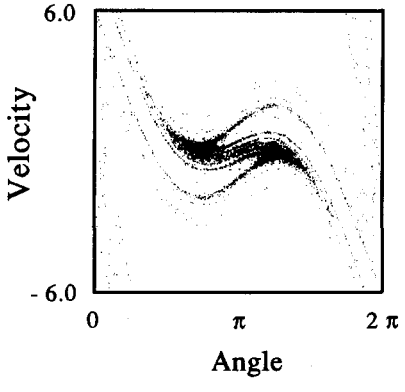

Fig. 15. Basin of attraction for the flutter mode with $Q=5$, $\epsilon=0.520$, $\Omega=11$.

ACKNOWLEDGMENTS

J. A. B. and H. J. T. S. received financial support from the Natural Sciences and Engineering Research Council of Canada. N. G-J was supported by the Otto Mønsteds Fond.

[a]Present address: Department of Applied Physics, Stanford University.

[1]H. C. Corben and P. Stehle, *Classical Mechanics* (Wiley, New York, 1960), 2nd ed., pp. 67–69.
[2]B. van der Pol and M. J. O. Strutt, "On the stability of the solutions of Mathieu's equation," Phil. Mag. **5**, 18–38 (1928).
[3]D. J. Ness, "Small oscillations of a stabilized, inverted pendulum," Am. J. Phys. **35**, 964–967 (1967).
[4]F. M. Phelps, III and J. H. Hunter, Jr., "An analytical solution of the inverted pendulum," Am. J. Phys. **33**, 285–295 (1965).
[5]F. M. Phelps, III and J. H. Hunter, Jr., "Reply to Joshi's comments on a damping term in the equations of motion of the inverted pendulum," Am. J. Phys. **34**, 533–535 (1966).
[6]M. H. Friedman, J. E. Campana, L. Kelner, E. H. Seeliger, and A. L. Yergey, "The inverted pendulum: A mechanical analog of the quadrupole mass filter," Am. J. Phys. **50**, 924–931 (1982).
[7]M. M. Michaelis, "Stroboscopic study of the inverted pendulum," Am. J. Phys. **53**, 1079–1083 (1985).
[8]J. Miles, "Directly forced oscillations of an inverted pendulum," Phys. Lett. **A133**, 295–297 (1988).
[9]J. A. Blackburn, S. Vik, B. Wu, and H. J. T. Smith, "Driven pendulum for studying chaos," Rev. Sci. Instrum. **60**, 422–426 (1989).
[10]N. W. McLachlan, *Theory and Application of Mathieu Functions* (Oxford U.P., New York 1951), pp. 39–41.
[11]J. J. Stoker, *Nonlinear Vibrations in Mechanical and Electrical Systems* (Wiley/Interscience, New York, 1966), pp. 202–213.
[12]C. Hayashi, *Nonlinear Oscillations in Physical Systems* (Princeton U.P., NJ, 1985), pp. 86–93.
[13]Equation (71) of Ref. 4 corresponds exactly to our Eq. (5). Equation (72) of Ref. 4 is equivalent, in our notation, to $\epsilon=0.450+2.22/\Omega^2$
[14]L. D. Landau and E. M. Lifshitz, *Mechanics* (Pergamon, New York, 1976), 3rd ed., pp. 93–95.
[15]Francis C. Moon, *Chaotic Vibrations* (Wiley, New York, 1987), p. 94.
[16]J. E. Marsden and M. McCracken, *The Hopf Bifurcation and its Applications* (Springer Verlag, New York, 1976).
[17]B. H. Tongue, "On obtaining global nonlinear system characteristics through interpolated cell mapping," Physica **28D**, 401–408 (1987).
[18]B. H. Tongue and K. Gu, "A theoretical basis for interpolated cell mapping," SIAM J. Appl. Math. **48**, 1206–1214 (1988).
[19]G. L. Baker and J. P. Gollub, *Chaotic Dynamics* (Cambridge U.P., Cambridge, UK, 1990).
[20]A. H. MacDonald and M. Plischke, "A study of the driven damped pendulum: Application to Josephson junctions and charge density wave systems," Phys. Rev. B **27**, 201–211 (1983).
[21]R. W. Leven, B. Pompe, C. Wilke, and B. P. Koch, "Experiments on periodic and chaotic motions of a parametrically forced pendulum," Physica **16D**, 371–384 (1985).